

Typical growth behavior of the out-of-time-ordered commutator in many-body localized systems

Juhee Lee, Dongkyu Kim, and Dong-Hee Kim*

*Department of Physics and Photon Science, School of Physics and Chemistry,
Gwangju Institute of Science and Technology, Gwangju 61005, Korea*

We investigate the typicality of the growth behavior of the out-of-time-ordered commutator (OTOC) in the many-body localized (MBL) quantum spin chains across random disorder realizations. In the MBL phase of the Heisenberg XXZ chain, we find that the estimate of the OTOC fluctuates significantly with the disorder realizations at the intermediate times of the main growth. Despite the consequent failure of the disorder average in the MBL phase, we argue that the characteristic behavior of the OTOC growth can still be identified by going through individual disorder realizations. We find that a power-law-type growth behavior appears typically after a disorder-dependent relaxation period, which is very close to the t^2 form derived in the effective Hamiltonian of a fully MBL system. The characteristic growth behavior observed at an individual disorder realization is robust in our tests with various state preparations and also verified in another MBL system of the random-transverse-field quantum Ising chain in a uniform longitudinal field.

I. INTRODUCTION

The out-of-time-ordered (OTO) commutator and correlator [1, 2] have attracted much attention recently because of their promising applications to the diagnosis of information scrambling [3–6] in the dynamics of quantum many-body systems. For two unitary operators \hat{W} and \hat{V} that are initially local at different positions, the OTO commutator is defined as the expectation value of their squared commutator,

$$C(t) = \frac{1}{2} \langle [\hat{W}(t), \hat{V}]^\dagger [\hat{W}(t), \hat{V}] \rangle, \quad (1)$$

which is often rewritten as $C(t) = 1 - \text{Re}[F(t)]$ in terms of the corresponding OTO commutator $F(t) = \langle \hat{W}^\dagger(t) \hat{V}^\dagger \hat{W}(t) \hat{V} \rangle$. The evaluation of $\langle \dots \rangle \equiv \text{Tr}[\hat{\rho} \dots]$ depends on the density matrix $\hat{\rho}$ of a pure or mixed state prepared for measurement. While the two distant operators commute with each other initially, $\hat{W}(t)$ in time evolution can be highly non-local in the presence of interactions, breaking the initial commutativity due to an overlap with \hat{V} . The growth of $C(t)$ can thus quantify such scrambling of information that spreads across nonlocal degrees of freedom. The characterization of quantum dynamics by using the OTO commutator and correlator has been the subject of intense study in systems ranging from a black hole [7–10] and Sachdev-Ye-Kitaev-type models [11–15] to various condensed matter models of chaotic [16–33] and non-chaotic [34–48] systems. Measurement protocols have been proposed [49–54], and there are recent advances in experimental measurements using nuclear spins of molecules [55], trapped ions [56], and ultracold gases [57].

One of the fundamental questions on the growth behavior of the OTO commutator may be whether there exists a characteristic form that can distinguish systems between different classes of information scrambling. In a chaotic system, $C(t)$ grows very fast, which is often described by the exponential behavior with the Lyapunov exponent. In the absence of chaos, the growth of $C(t)$ can be much slower or even absent.

In particular, measuring $C(t)$ in disordered systems may distinguish many-body localization [58–61] from Anderson localization [62]. Both of them arrest particle transport, but in many-body localized (MBL) systems, the dephasing effects due to the interactions allow the spreading of quantum information, leading to characteristic dynamics [63–66] including slowly growing $C(t)$ [40–47].

The specific question that we want to address here is how typical a particular slow-growth behavior of $C(t)$ is across different disorder realizations in a disordered MBL system. In the effective “1-bit” Hamiltonian of a fully MBL system, it was shown that the growth of the disorder average $\overline{C(t)}$ proceeds as $\overline{C(t)} \sim t^2$ at early times, and then it is saturated with a power-law decaying second moment at late times [40–42]. However, beyond the effective Hamiltonian, it is not entirely clear how universal this particular power-law form of the growth is in more realistic models and whether or not it can characterize a wider range of the disordered MBL systems.

In this paper, we investigate the time evolution of $C(t)$ in two quantum spin models of the Heisenberg XXZ and mixed-field Ising chains across their random disorder realizations. We find that in the MBL phase, the disorder average cannot properly show the behavior of $C(t)$ because of the large deviations across the disorder realizations. The estimate of $C(t)$ at an intermediate time exhibits a bimodal distribution, which is in contrast to a singly peaked distribution evolving in the ergodic side. However, by going through individual disorder realizations, we find that the systems typically undergo common stages of the OTO commutator growth. At very early times, $C(t)$ shows an intrinsic power-law growth, and it is shortly relaxed by the period of an oscillatory plateau that makes an offset at a small value of C for the main stage of the growth emerging at intermediate times.

For an individual disorder realization, the main growth of $C(t)$ turns out to be often very close to the t^2 form, while it appears with an offset and a time delay that fluctuate very much with disorder realizations. Based on numerical observations, we argue that the growth can be characterized as $C(t) \sim c_0 + \epsilon t^2$ with an offset c_0 at intermediate times by combining the coarse-grained effect of fast dynamics and the slow t^2 contribution emerging from the effective Hamiltonian. We

* dongheekim@gist.ac.kr

also observe that the growth behavior at a fixed disorder realization is insensitive to the choice of the state $\hat{\rho}$ that we examine for the measurement of $C(t)$.

This paper is organized as follows. In Sec. II, we revisit the effective 1-bit Hamiltonian for the OTO commutator growth behavior at a given disorder configuration. In Sec. III, we present the typicality and deviations of the growth behavior across random disorder realizations in the Heisenberg XXZ model. The representativeness of disorder average is examined, and the growth behavior is characterized at an individual disorder realization. In Sec. IV, we verify the appearance of the characteristic growth form in the mixed-field Ising model. The summary and conclusions are given in Sec. V.

II. THE PHENOMENOLOGICAL “L-BIT” MODEL

Let us briefly revisit the behavior of the OTO commutator in the phenomenological model of a fully MBL system. The effective “1-bit” Hamiltonian [67–69] is written as

$$\mathcal{H} = \sum_i h_i \hat{\tau}_i^z + \sum_{\{i,j\}} J_{ij} \hat{\tau}_i^z \hat{\tau}_j^z + \sum_{\{i,j,k\}} K_{ijk} \hat{\tau}_i^z \hat{\tau}_j^z \hat{\tau}_k^z + \dots, \quad (2)$$

where $\hat{\tau}_i^z$ is the z component of the Pauli operator for a dressed spin-1/2 localized at site $i \in [1, L]$ in the chain of length L . The summation runs over the sets of unique site indices. The coefficients are given as random variables for the multispin interactions which have characteristic strength decaying exponentially with distance between the farthest-apart spins. The OTO correlator $F(t)$ was derived previously for the operator choice of $\hat{W} = \hat{\tau}_a^x$ and $\hat{V} = \hat{\tau}_b^y$ [40–42]. From the previous results, we can write down the corresponding OTO commutator $C(t)$ for a given disorder realization as

$$C(t) = 1 - \text{Re} \left[\langle \exp(it 4 \hat{J}_{ab}^{\text{eff}} \hat{\tau}_a^z \hat{\tau}_b^z) \rangle \right] \quad (3)$$

$$\simeq 1 - \cos(4t \langle \hat{J}_{ab}^{\text{eff}} \rangle) \exp \left[-8t^2 (\langle [\hat{J}_{ab}^{\text{eff}}]^2 \rangle - \langle \hat{J}_{ab}^{\text{eff}} \rangle^2) \right].$$

The effective interaction operator $\hat{J}_{ab}^{\text{eff}}$ for the spins at a and b can be written by collecting all terms involving a and b as

$$\hat{J}_{ab}^{\text{eff}} = J_{ab} + \sum'_k K_{abk} \hat{\tau}_k^z + \sum'_{\{k,l\}} Q_{abkl} \hat{\tau}_k^z \hat{\tau}_l^z + \dots, \quad (4)$$

where the sites a and b are excluded in the primed sums.

The early-time growth of $C(t)$ shows the quadratic behavior indicated by the leading-order term of

$$C(t) = 8 \langle [\hat{J}_{ab}^{\text{eff}}]^2 \rangle t^2 + O(t^4). \quad (5)$$

Within the effective Hamiltonian, this t^2 growth form of $C(t)$ may characterize the MBL systems and is qualitatively independent of a state prepared for the measurement and a particular disorder realization as long as $\hat{J}_{ab}^{\text{eff}}$ is essential.

The late-time behavior of $C(t)$ shows oscillations with a period and decay factor that depend on the disorder realization and the state used for measurement. In the disorder average, it is dephased and saturates around $C = 1$ [40, 42]. However, it is worth noting a particular type of the measurement

with an eigenstate in which all moments of $\hat{J}_{ab}^{\text{eff}}$ are the same, where the OTO commutator becomes a simple oscillation as $C_{\text{eig}}(t) = 1 - \cos(4t \langle \hat{J}_{ab}^{\text{eff}} \rangle)$. In this special case, the t^2 growth is a transient behavior of the simple oscillation with a long period $\pi/2 \langle \hat{J}_{ab}^{\text{eff}} \rangle$ given by the effective interaction.

While the early-time t^2 behavior is persistent at any given disorder realization in this phenomenological model, quantitative fluctuations across different realizations of disorders can also be important. Here we briefly discuss the shape of the probability distribution $P(C)$ measured at a given early time t over random disorder realizations for the later comparison with the results in more realistic models. For simplicity, let us borrow the uniform distribution $[-2^{-1/2} e^{-1/\zeta}, 2^{-1/2} e^{-1/\zeta}]$ from Ref. [42] for a random interaction term with the farthest-apart spins of distance l in Eq. (2) to produce the effective interaction with a decay length ζ . For the evaluation of $C(t)$, we consider the two particular types of the states that include the maximally mixed state $\hat{\rho} \propto \mathbb{1}$ at infinite temperature and the pure state given by an eigenstate. In both cases, the central limit theorem works straightforwardly, providing a Gaussian shape of $P(C)$ with the average and width increasing as t^2 for the case of the maximally mixed state and $P(C) \sim C^{-1/2} \exp(-C/c_t)$ with the cutoff c_t increasing as t^2 for the case of an eigenstate.

The measurement at infinite temperature seems to be ideal in the sense that it gives the Gaussian distribution centered at the disorder average moving as t^2 . However, for a general state, the location of the average may not indicate a typical value as exemplified in the heavy-tailed distribution in the evaluation with an eigenstate. Nevertheless, in the phenomenological model, one can obtain the qualitatively correct growth of $C(t)$ from the disorder average, no matter how severe the fluctuations are, since every disorder realization produces the same early-time t^2 behavior starting from $t = 0$.

This ideal situation that allows $C(t) \propto t^2$ to be observed at an arbitrarily early time implies that the particular process of the scrambling is the only dynamics in the 1-bit model. In more realistic MBL systems, it is reasonable to assume the presence of other system-specific dynamics that may coexist with, or perhaps obscure, the characteristic scrambling behavior expected. Thus, it is a nontrivial question to ask whether or not one can see in practice the t^2 behavior beyond the effective Hamiltonian. In the next sections, we will present how the OTO commutator growth develops in the disordered XXZ and mixed-field Ising models.

III. RANDOM-FIELD HEISENBERG XXZ MODEL

We first consider the spin-1/2 Heisenberg XXZ chain with a random Zeeman field given by the Hamiltonian,

$$\mathcal{H} = - \sum_{i=1}^{L-1} [\hat{S}_i^x \hat{S}_{i+1}^x + \hat{S}_i^y \hat{S}_{i+1}^y + J_z \hat{S}_i^z \hat{S}_{i+1}^z] + \sum_{i=1}^L h_i \hat{S}_i^z, \quad (6)$$

where the random field h_i is uniformly sampled from the range of $[-\eta, \eta]$. The energy unit and \hbar are set to be unity. It is known that many-body localization occurs in this system

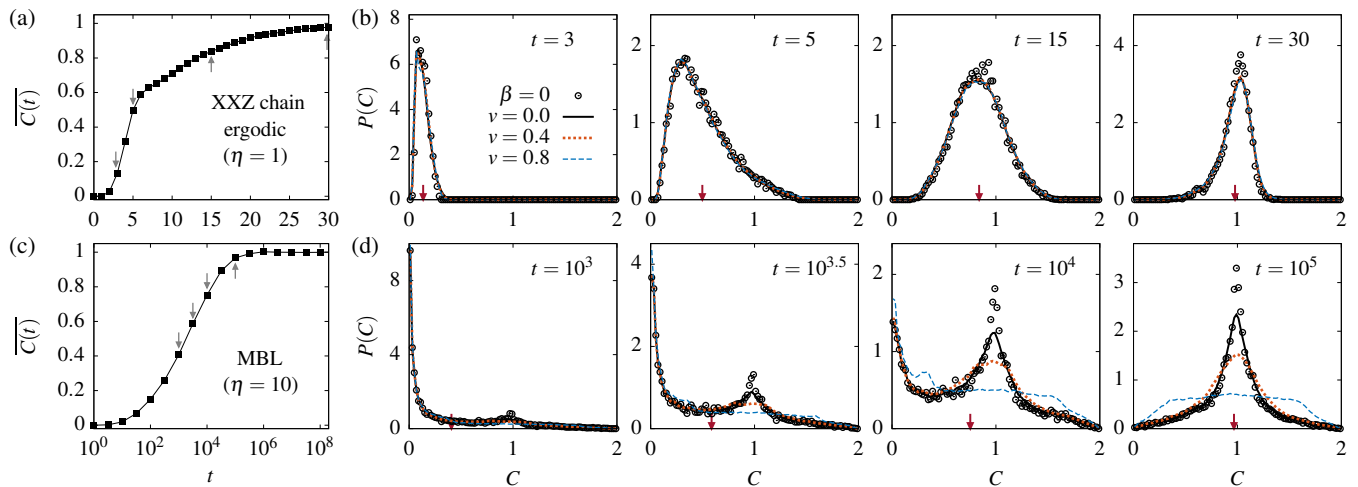


FIG. 1. Probability distribution of the OTO commutator measured along the growth in the random-field Heisenberg XXZ chain. The disorder average $\overline{C(t)}$ and the distribution $P(C)$ estimated at selected times over the disorder realizations are displayed for the disorder strengths of $\eta = 1$ and $\eta = 10$ in the ergodic (a, b) and MBL (c, d) phases, respectively. The OTO commutator C is measured with the maximally mixed state at infinite temperature ($\beta = 0$) and the random pure states at several values of v . The locations of the disorder average are indicated by the arrows in (b) and (d) which are not affected by the choice of the state. The distributions are estimated with 10000 disorder realizations and averaged over 100 random states at each v in the system of length $L = 12$.

for nonzero interactions $J_z \neq 0$ and strong enough disorder strength η [70–74]. Here we fix the interaction at $J_z = 0.2$ and consider the two particular values of the disorder strength, $\eta = 1$ and $\eta = 10$, where the system belongs to the ergodic and MBL phases, respectively. We define the OTO commutator $C(t)$ by choosing the Pauli spin operators as $\hat{W} = \hat{\sigma}_4^x$ at site $i = 4$ and $\hat{V} = \hat{\sigma}_1^x$ at one end of the chain. We employ the exact diagonalization for the numerical calculations of $C(t)$ in the systems of length $L = 12$.

For the measurement of $C(t)$, we mainly consider the maximally mixed state $\hat{\rho} = \mathbb{1}/2^L$ at infinite temperature but also examine the random pure state $\hat{\rho} = |\Psi_v\rangle\langle\Psi_v|$ given by

$$|\Psi_v\rangle = \bigotimes_{i=1}^L \left(\cos \frac{\theta_i}{2} |\uparrow\rangle + e^{i\phi_i} \sin \frac{\theta_i}{2} |\downarrow\rangle \right) \quad (7)$$

which is a product of local spin states sampled on the Bloch sphere. We follow the scheme of Ref. [75] where ϕ_i is a uniform random variable in $[0, 2\pi)$, and the polar angle θ_i is restricted for $\cos \theta_i$ to be either v or $-v$ at each site. At $v = 0$, $|\Psi\rangle$ is the sum of all σ_z -basis vectors with random phases, sharing the constant diagonal part of $\hat{\rho}$ with the maximally mixed state. On the other hand, $v = 1$ selects one of the σ_z -basis vectors that would be locally similar to an eigenstate in the strong-disorder limit. Thus, varying v may provide a systematic way to demonstrate the dependence of the estimate of $C(t)$ on the state preparations.

We find that the probability distribution $P(C)$ of the OTO commutator shows contrasting behavior between the ergodic and MBL phases of the disordered XXZ chain. Figure 1 presents the time evolution of $P(C)$ along the main growth of the commutator measured over 10000 random disorder realizations. In the ergodic phase, a singly peaked distribution moves from $C = 0$ to 1 as the time goes, and its shape is inde-

pendent of the parameter v of the random pure states used for measurement, which also agrees well with the shape observed with the infinite-temperature state.

In contrast, in the MBL phase, the distribution $P(C)$ turns out to be bimodal at the intermediate times of the main growth in the measurement with the infinite-temperature state and random pure states with small v . In the time evolution of $P(C)$, the population migrates from one peak at $C \approx 0$ to the other at $C \approx 1$. The shape depends on the parameter v since the late-time saturation behavior varies with v . The disorder average of $C(t)$ does not depend on the choice of the state, which, however, does not imply that the disorder average presents a typical behavior of $C(t)$. The bimodal distributions observed at the intermediate times of the growth indicate that the disorder average is not physically meaningful in this regime. Indeed, the growth of the disorder average is quite different from the characteristic behavior observed at an individual disorder realization which we present below.

The emergence of the bimodality in $P(C)$ may work as an empirical indicator of the localization transition in the XXZ chain. Figure 2 displays the transition in the shape of $P(C)$ with the disorder strength η examined with the average given at $\overline{C} \approx 0.6$. As η increases, the top of the unimodal distribution in the ergodic phase becomes flat, and then double peaks start to develop at a larger η . It turns out that the range of η in which the transition in the distribution shape occurs is consistent with the area of the localization transition indicated by the average gap ratio [59, 74] which we evaluate for our parameter $J_z = 0.2$ in Fig. 2(b).

Since $P(C)$ in the MBL phase of the XXZ model is very different from the Gaussian distribution found in the effective 1-bit model, natural questions are then what are the origins of the bimodal distribution and how it is related to the slow characteristic dynamics of $C(t)$ found in the effective model. In

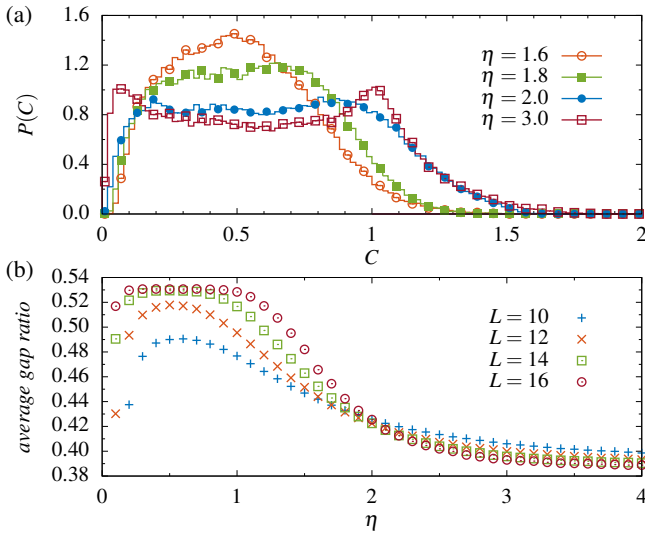


FIG. 2. OTO commutator distribution around the localization transition in the XXZ chain. (a) Distribution $P(C)$ measured at $\overline{C(t)} \approx 0.6$ with the infinite-temperature state. (b) Average gap ratio computed for eigenvalues E within the distance $\Delta e = 0.1$ from the spectrum center $e = 0.5$, where $e \equiv (E - E_{\min}) / (E_{\max} - E_{\min})$, and $E_{\max(\min)}$ is the largest (smallest) eigenvalue.

order to address these questions, we look into the growth behavior of $C(t)$ at the level of individual disorder realizations. It turns out that the early-time stage of $C(t)$ is distinguished from the main growth stage, giving a waiting period at a very small C after which the main growth starts to become visible. The time period of each growth stage shows large deviations between different disorder realizations, contributing to the slowly decreasing population at $C \approx 0$ and the broad distribution over intermediate values of C with another peak appearing due to the saturation around $C \approx 1$.

While the disorder average at a given time is largely influenced by the populations of $C \approx 0$ and $C \approx 1$, the main growth behavior observed at an individual disorder realization shows the characteristic feature expected from the effective model. Figure 3(a) schematically describes the behavior observed at each stage. At very early times, $C(t)$ shows the initial power-law growth behavior of t^6 for our choice of the two local operators with distance $r = 3$. The initial growth is relaxed shortly at the level of small C , leading to the oscillatory relaxation plateau. The main growth emerges with another yet characteristic power-law type behavior, which becomes saturated with long-period oscillations at late times.

The initial power-law growth is an intrinsic feature of the base spin model and is not related to many-body localization. The early-time behavior can be easily understood from the series expansion of the commutator $[\hat{\sigma}_{r+1}^x(t), \hat{\sigma}_1^x]$. Following the same procedures of Ref. [34], the Baker-Campbell-Hausdorff expansion of $\hat{\sigma}_{r+1}^x(t)$ provides

$$\hat{\sigma}_{r+1}^x(t) = \hat{\sigma}_{r+1}^x + it[\mathcal{H}, \hat{\sigma}_{r+1}^x] + \frac{(it)^2}{2!}[\mathcal{H}, [\mathcal{H}, \hat{\sigma}_{r+1}^x]] + \dots, \quad (8)$$

where the first appearance of the term that does not commute

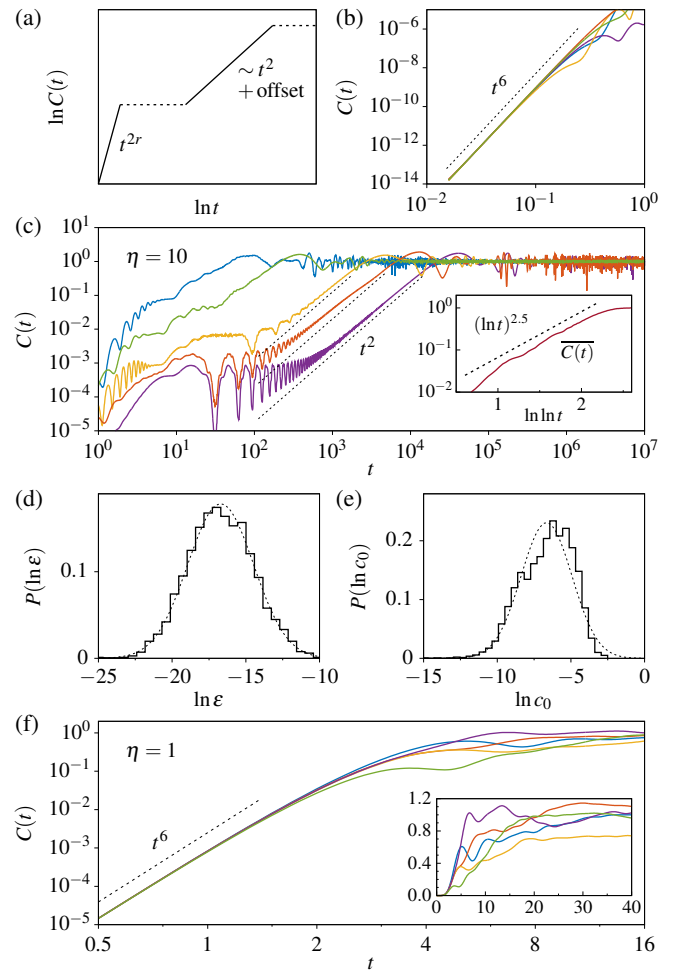


FIG. 3. Growth of the OTO commutator in the MBL phase of the XXZ chain. (a) Schematic of the power-law behaviors (solid lines) and oscillatory relaxations (dotted lines) observed at an individual disorder realization. Examples of five selected disorder realizations are shown for (b) the early-time and (c) intermediate-time growth of $C(t)$ at $\eta = 10$ measured with the infinite-temperature state in the system of $L = 12$. The inset of (c) shows the disorder average $\overline{C(t)}$. The distributions of (d) ε and (e) c_0 from the fits of $C(t) = c_0 + \varepsilon t^2$ to the main growth parts are compared with the log-normal ones (dotted lines) having the same averages and variances. (f) Examples of $C(t)$ at $\eta = 1$ in the ergodic phase given for comparison.

with $\hat{\sigma}_1^x$ is associated with t^r , and therefore, the squared commutator grows as t^{2r} at very early times. While this initial power-law form has been derived and discussed previously as a general property of spin chains [29, 34, 48], it is still important to recall that the leading-order t^{2r} term is independent of the disorders and can appear without any contribution of the interaction that is essential to the MBL phase.

The second growth behavior of a power-law type that leads to a main increase in C becomes visible after the plateau of oscillatory relaxations that suppress the initial t^{2r} growth. Figure 3(c) shows typical examples of the intermediate-time quadratic growth behavior at individual disorder realizations that are drastically different from the behavior of the disorder

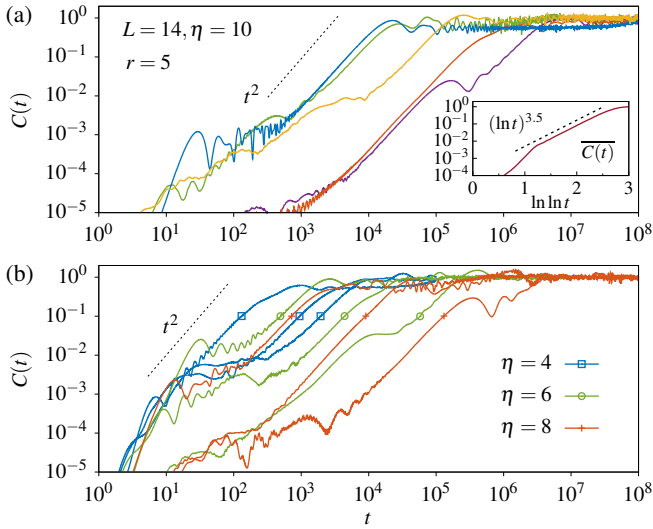


FIG. 4. Verification of the main power-law growth in a larger system of the disordered XXZ chain. The OTO commutator with the operator distance $r = 5$ is considered in the systems of length $L = 14$. (a) Five selected examples of the t^2 growth behavior at $\eta = 10$. The inset of (a) indicates the disorder average $\overline{C(t)}$. (b) Examples of the t^2 behavior at weaker disorder strengths in the MBL phase.

der average that looks like $\overline{C(t)} \sim (\ln t)^{2.5}$. The behavior of $\overline{C(t)}$ is not universal and depends on r and the model systems as shown in Figs. 4 and 7. Unlike the effective model, the characteristic behavior can hardly survive in the disorder average done at a given time that includes different stages of growth because of the large fluctuations of their time periods, and thus the quadratic growth is only identifiable in the level of individual disorder realizations.

While the intermediate-time growth often shows an excellent fit to the t^2 form found in the 1-bit model, we find that the main growth is better characterized as $C(t) \approx c_0 + \epsilon t^2$ with an offset c_0 representing the contributions of short-time dynamics indicated by the relaxation plateau. A large value of the plateau makes a poor fit to the strict form of t^2 as can be seen in the examples given in Fig. 3(c). Several dynamic processes of different time scales may coexist in the OTO commutator. In the sense of a fixed-point Hamiltonian, the t^2 component may represent the long-time scrambling dynamics while the coarse-grained effects of all faster dynamics appear as a constant offset in the scale of intermediate and later times.

Figures 3(d) and 3(e) display the distributions of c_0 and ϵ in the logarithmic scale. In particular, the one for ϵ contrasts with the Gaussian distribution of the corresponding quantity $\langle [\hat{J}^{\text{eff}}]^2 \rangle$ in the 1-bit model. Given that $\langle [\hat{J}^{\text{eff}}]^2 \rangle$ was an addition of random variables at the maximally mixed state, the log-normal shape could suggest that ϵ would come from a multiplicative process with random disorders, characterizing the large deviations between individual disorder realizations.

Figure 4 verifies the power-law behavior of $C(t)$ for a longer operator distance $r = 5$ in the system of $L = 14$ while we have mainly considered $r = 3$ and $L = 12$. The power-law behavior is demonstrated at several values of the disorder strength η

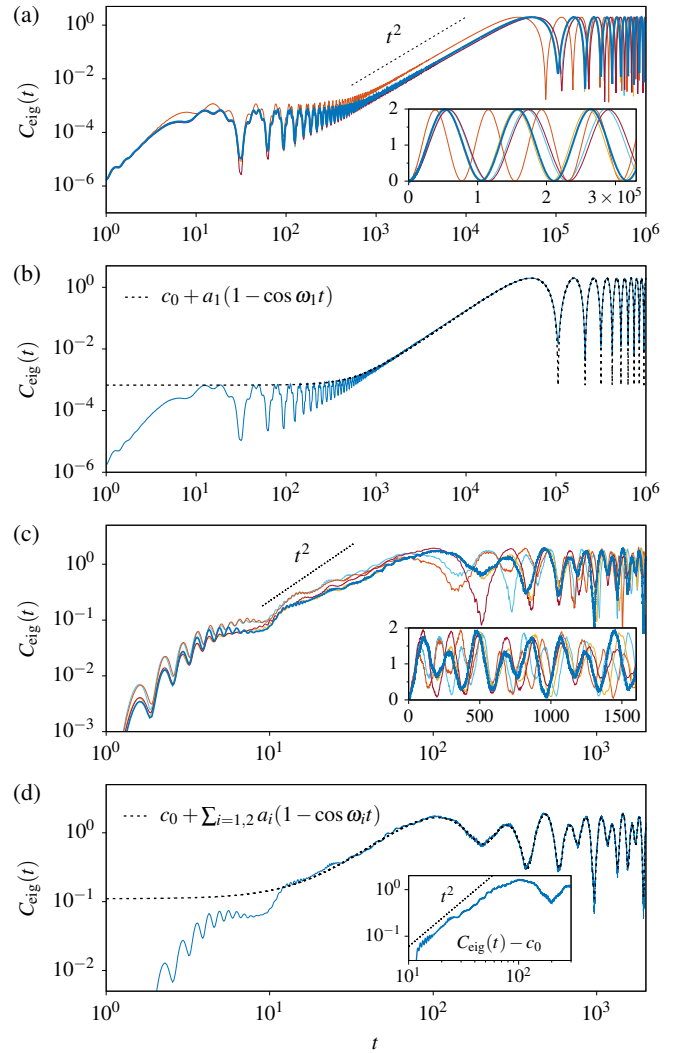


FIG. 5. OTO commutator measured with eigenstates at two given disorder realizations. The disorder realizations chosen for (a, b) and (c, d) are associated with the rightmost and leftmost lines in Fig. 3(c), respectively, which contrast the cases of an excellent fit to the t^2 form and a poor power-law fit. The lines displayed in (a) and (c) are different measurement with five eigenstates randomly chosen from the middle of the spectrum, among which one line is presented again in (b) and (d) for a fit to the empirical formula of the $(1 - \cos \omega_i t)$ oscillations with an offset c_0 .

of the MBL side. The time scale of the main growth stage tends to increase with r and η , which influences the visibility of the power law in a finite system. At a weak η close to the transition, one would need a very large r for the main growth time scale to become separated from the early-time processes. The t^2 growth is thus more pronounced in practice at stronger η in a system with small r , and thus we mainly consider the deep MBL regime at $\eta = 10$ in the XXZ chain.

A pure-state measurement with an eigenstate at a given disorder realization may demonstrate more clearly the essential role of the slowest dynamics in the MBL phase to the power-law growth at intermediate times and the long-time behavior

appearing at late times. For a given eigenstate $|\alpha\rangle$, one can express the OTO commutator $C_{\text{eig}}(t)$ explicitly as

$$C_{\text{eig}}(t) = 1 - \text{Re} \left[\sum_{\beta, \gamma, \delta} e^{it(E_\alpha - E_\beta + E_\gamma - E_\delta)} s_{\alpha\beta\gamma\delta} \right], \quad (9)$$

where $s_{\alpha\beta\gamma\delta} = \langle \alpha | \hat{\sigma}_3^x | \beta \rangle \langle \beta | \hat{\sigma}_0^x | \gamma \rangle \langle \gamma | \hat{\sigma}_3^x | \delta \rangle \langle \delta | \hat{\sigma}_0^x | \alpha \rangle$, and E_α is the energy of the eigenstate $|\alpha\rangle$. Inspired by the effective Hamiltonian, the long-period oscillations in the MBL phase may be determined by a few smallest magnitudes of $(E_\alpha - E_\beta + E_\gamma - E_\delta)$ with a dominant $s_{\alpha\beta\gamma\delta}$. Then, one can write down the late-time expression of $C_{\text{eig}}(t)$ as

$$C_{\text{eig}}(t) \approx c_0 + \sum_{i=1}^n c_i (1 - \cos \omega_i t), \quad (10)$$

if ω_i is well separated from the larger frequencies that are coarse-grained in an offset c_0 for the low-resolution description at intermediate and late times. In $C_{\text{eig}}(t)$, the t^2 form appears in a transient behavior of the cosine term as found in the effective 1-bit Hamiltonian with an eigenstate.

Figure 5 demonstrates the existence of dominant long-period modes by providing the two particular examples of the best and worst fits to the strict t^2 form chosen among the cases shown in Fig. 3(c). In the one with the best fit, it turns out that $C_{\text{eig}}(t)$ at intermediate and late times can be described with just one frequency in Eq. (10). In the other one, the contributions of two frequencies are dominant with a relatively high offset, which has caused the poor fit to the strict power-law form at intermediate times if the offset is not considered. In both cases, we have not observed qualitative variations with different choices of an eigenstate while the value of the frequency depends on the eigenstate. The number of dominant modes and the separation between the frequencies depend mainly on the disorder realization.

The intermediate-time growth behavior, $C(t) \sim c_0 + \epsilon t^2$, observed at an individual disorder realization remains the same in all our choices of the state for measurement. We have examined the random pure states at various values of v . The one at $v = 0$ is essentially the same as $C(t)$ obtained with the maximally mixed state at the infinite temperature while the one at $v = 1$ is very similar to the measurement with an eigenstate. These will be shown explicitly in the next section, where the observation of the characteristic behavior in the MBL phase is verified in the mixed-field Ising model.

IV. MIXED-FIELD ISING MODEL

Another MBL system that we consider is the random-transverse-field quantum Ising chain in a uniform longitudinal field [42]. The Hamiltonian is given as

$$\mathcal{H} = - \sum_{i=1}^{L-1} \hat{\sigma}_i^z \hat{\sigma}_{i+1}^z - \sum_{i=1}^L h_i \hat{\sigma}_i^x - h_z \sum_{i=1}^L \hat{\sigma}_i^z, \quad (11)$$

where the random transverse field h_i is sampled from the uniform distribution in $[-W, W]$. The strengths of the random

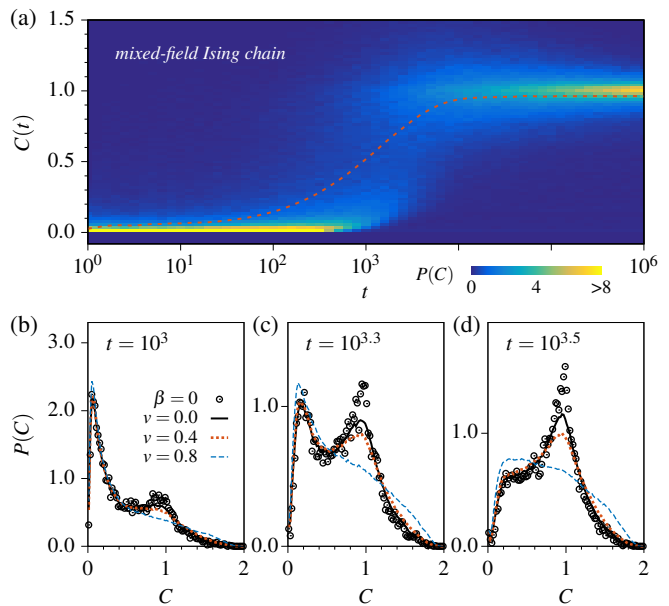


FIG. 6. Probability distribution of the OTO commutator in the mixed-field Ising chain. (a) The distribution $P(C)$ is visualized with the color code for the probability density of the OTO commutator $C(t)$ measured at a given time t across 10000 disorder realizations with the infinite-temperature state ($\beta = 0$). The dotted line indicates the disorder average $\overline{C(t)}$. The random pure-state estimates for $v = 0, 0.4, 0.8$ are compared with the infinite-temperature estimate in (b-d) at selected times along the main growth of $C(t)$.

field and the uniform longitudinal field are fixed at $W = 10$ and $h_z = 0.1$, respectively. The chain length $L = 12$ is considered. The OTO commutator is defined with the operators $\hat{W} = \hat{\sigma}_i^z$ and $\hat{V} = \hat{\sigma}_0^z$ by following Ref. [42]. The maximally mixed state and random pure states are considered for measurement, where the pure state is defined analogously as

$$|\Psi_v\rangle = \bigotimes_{i=1}^L \left(\cos \frac{\theta_i}{2} |x; +\rangle + e^{i\phi_i} \sin \frac{\theta_i}{2} |x; -\rangle \right) \quad (12)$$

with the basis $|x; \pm\rangle$ of the Pauli operator $\hat{\sigma}^x$ along the axis of the random transverse fields.

As we have seen in the MBL phase of the XXZ chain, the disorder average $\overline{C(t)}$ in the mixed-field Ising chain also fails to represent the growth behavior of the OTO commutator $C(t)$ as indicated by Fig. 6(a). The probability distributions of $C(t)$ measured across the random disorder realizations are very similar to those that we have observed in the XXZ chain. The main growth of $C(t)$ appears with a time delay that fluctuates significantly across the disorder realizations, which leads to large deviations in the distribution $P(C)$. In particular, at intermediate times, $P(C)$ shows a clear double-peak structure when measured with the infinite-temperature state and the random pure state at $v = 0$, which agrees well with our previous observation in the XXZ chain.

The characterization of the growth behavior of $C(t)$ at an individual disorder realization shows excellent agreement with the multiple stages observed in the MBL phase of the disor-

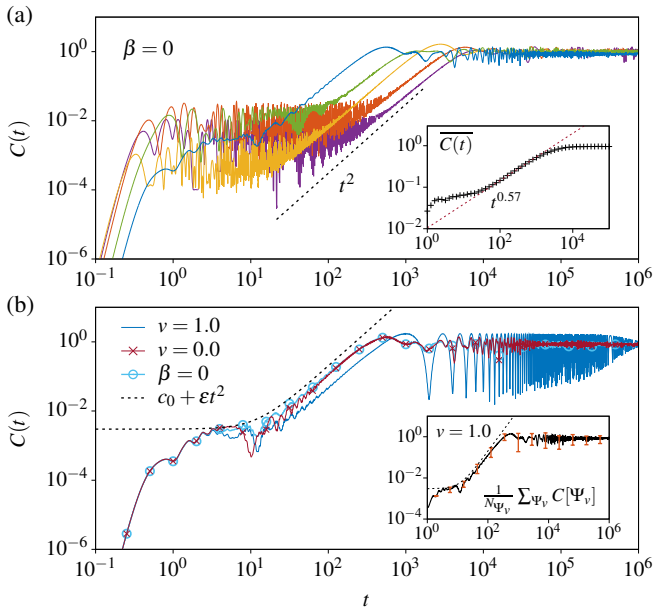


FIG. 7. OTO commutator in the mixed-field Ising chain at an individual disorder realization. (a) The growth of $C(t)$ of the infinite-temperature estimate ($\beta = 0$) is plotted for five selected disorder realizations. The inset of (a) shows the disorder average $\overline{C(t)}$ calculated over 10000 realizations for comparison. (b) The random-pure-state estimate is presented for $\nu = 0.0$ and 1.0 at a fixed disorder realization chosen from (a). The inset of (b) presents the averages (solid lines) and standard deviations (error bars) measure over 100 generations of the random states drawn at $\nu = 1$.

dered XXZ chain. Figure 7 presents typical examples that show the initial power-law growth, the plateau of oscillatory relaxations, the main growth of a power-law form at intermediate times, and then the saturation around $C \approx 1$ in the late times. In the expansion of the commutator in the small time limit, one can easily show that the initial growth of $C(t)$ follows an intrinsic form of $C(t) \sim t^{4r+2}$, where $r = 2$ for our choice of \hat{W} and \hat{V} . A slight difference from the XXZ model is that the random transverse fields contribute to the t^{4r+2} term, but it is still independent of the longitudinal field h_z that triggers many-body localization in this system.

The intermediate-time main growth behavior also verifies the characterization of the power-law form $C(t) \sim c_0 + \epsilon t^2$ with an offset c_0 that is consistently observed in the different state preparations of the infinite-temperature state and the random pure states. Averaging over disorder realizations distorts the main growth behavior as seen in the inset of Fig. 7(a) because of the large deviations in the time period and level of the relaxation plateau setting the offset. On the other hand, at a fixed disorder, our tests with different random states indicate that the main growth behavior of the power-law form is very robust in the intermediate-time regime.

At a fixed disorder, the deviations between different random generations of the pure state appear mainly in the saturation stage at late times. For instance, in the case of $\nu = 1$, the $(1 - \cos \omega t)$ oscillations survive for a long period of time because of the significant participation of a single eigenstate.

While these long-period oscillations are dephased effectively by averaging over many random states at the same ν , the well-defined frequency of the oscillations at late times can be used for measuring an effective interaction. For a strong-disorder field, a single random pure state at $\nu = 1$ generated in the axis of the disorder field may provide an approximate estimate of $\langle \hat{j}^{\text{eff}} \rangle \propto \omega$ between the two local operators examined for the OTO commutator growth behavior.

V. SUMMARY AND CONCLUSIONS

In conclusion, our results suggest that in the MBL systems, there exists a typical power-law-like behavior in the main growth of the OTO commutator at intermediate times that can be observed in the level of an individual disorder realization. The onset time of the main growth shows large fluctuations across the disorder realizations, requiring the study of the OTO commutator growth to be constrained to each realization of disorders. For a fixed disorder configuration, the main growth characteristics at intermediate times are unaffected by different choices of the maximally mixed or random pure states prepared for the measurement.

We have examined two MBL systems of the Heisenberg XXZ chain with a random Zeeman field and the random-transverse-field Ising chain with a uniform longitudinal field. At an individual disorder realization, both show qualitatively the same behavior of the OTO commutator $C(t)$. The initial growth exhibits an intrinsic power law that is unrelated to many-body localization. The initial growth is shortly suppressed by the relaxation plateau, making an offset added up to the t^2 behavior that appears as the main growth of $C(t)$. We have argued that the dominantly slow components of the OTO commutator found at an eigenstate is the essence of the t^2 growth behavior as indicated in the effective Hamiltonian, while the fast components are coarse-grained in the offset c_0 of $C(t) \sim c_0 + \epsilon t^2$ observed at intermediate times.

The disorder average often works as a convenient tool to study a disordered system by reducing statistical noises. However, our calculations indicate that it may not generalize for $C(t)$ in the MBL systems. It turns out that the time scale and level of the relaxation plateau fluctuate severely across disorder realizations, preventing the disorder average from capturing the characteristic growth at intermediate times. Although the estimate of $C(t)$ may not be self-averaging, the typicality of the power-law behavior that we have identified at individual disorder realizations raises a possibility that one may still be able to characterize MBL systems with the OTO commutator just by testing a few samples of quenched disorders.

ACKNOWLEDGMENTS

This work was supported from the Basic Science Research Program through the National Research Foundation of Korea funded by the Ministry of Education (NRF-2017R1D1A1B03034669).

- [1] A. I. Larkin and Y. N. Ovchinnikov, Zh. Eksp. Teor. Fiz. **55**, 2262 (1968) [Sov. Phys. JETP **28**, 1200 (1969)].
- [2] A. Kitaev, Hidden Correlations in the Hawking Radiation and Thermal Noise, in *Fundamental Physics Prize Symposium* (Stanford University, California, USA, 2014).
- [3] D. N. Page, Phys. Rev. Lett. **71**, 1291 (1993).
- [4] P. Hayden and J. Preskill, J. High Energy Phys. **9** (2007) 120.
- [5] Y. Sekino and L. Susskind, J. High Energy Phys. **10** (2008) 65.
- [6] N. Lashkari, D. Stanford, M. Hastings, T. Osborne, and P. Hayden, J. High Energy Phys. **4** (2013) 22.
- [7] S. H. Shenker and D. Stanford, J. High Energy Phys. **3** (2014) 67.
- [8] D. A. Roberts, D. Stanford, and L. Susskind, J. High Energy Phys. **3** (2015) 51.
- [9] J. S. Cotler, G. Gur-Ari, M. Hanada, J. Polchinski, P. Saad, S. H. Shenker, D. Stanford, A. Streicher, and M. Tezuka, J. High Energy Phys. **5** (2017) 118.
- [10] S. Grozdanov, K. Schalm, and V. Scopelliti, Phys. Rev. Lett. **120**, 231601 (2018).
- [11] W. Fu and S. Sachdev, Phys. Rev. B **94**, 035135 (2016).
- [12] J. Maldacena and D. Stanford, Phys. Rev. D **94**, 106002 (2016).
- [13] Y. Gu, X.-L. Qi, and D. Stanford, J. High Energy Phys. **5** (2017) 125.
- [14] S. Banerjee and E. Altman, Phys. Rev. B **95**, 134302 (2017).
- [15] Y. Gu, A. Lucas, and X.-L. Qi, SciPost Phys. **2**, 18 (2017).
- [16] J. Maldacena, S. H. Shenker, and D. Stanford, J. High Energy Phys. **08** (2016) 106.
- [17] T. Scaffidi and E. Altman, arXiv:1711.04768.
- [18] H. Shen, P. Zhang, R. Fan, and H. Zhai, Phys. Rev. B **96**, 054503 (2017).
- [19] E. B. Rozenbaum, S. Ganeshan, and V. Galitski, Phys. Rev. Lett. **118**, 086801 (2017).
- [20] A. Bohrdt, C. B. Mendl, M. Endres, and M. Knap, New J. Phys. **19**, 063001 (2017).
- [21] A. A. Patel, D. Chowdhury, S. Sachdev, and B. Swingle, Phys. Rev. X **7**, 031047 (2017).
- [22] A. A. Patel and S. Sachdev, Proc. Natl. Acad. Sci. U.S.A. **114**, 1844 (2017).
- [23] D. Stanford, J. High Energy Phys. **10** (2016) 9.
- [24] D. Chowdhury and B. Swingle, Phys. Rev. D **96**, 065005 (2017).
- [25] I. Kukuljan, S. Grozdanov, and T. Prosen, Phys. Rev. B **96**, 060301(R) (2017).
- [26] D. J. Luitz and Y. Bar Lev, Phys. Rev. B **96**, 020406(R) (2017).
- [27] S. V. Syzranov, A. V. Gorshkov, and V. Galitski, Phys. Rev. B **97**, 161114(R) (2018).
- [28] Y.-L. Zhang, Y. Huang, and X. Chen, Phys. Rev. B **99**, 014303 (2019).
- [29] S. Xu and B. Swingle, arXiv:1802.00801.
- [30] V. Khemani, D. A. Huse, and A. Nahum, Phys. Rev. B **98**, 144304 (2018).
- [31] J. Rammensee, J. D. Urbina, and K. Richter, Phys. Rev. Lett. **121**, 124101 (2018).
- [32] I. García-Mata, M. Saraceno, R. A. Jalabert, A. J. Roncaglia, and D. A. Wisniacki, Phys. Rev. Lett. **121**, 210601 (2018).
- [33] Y. Alavirad and A. Lavasani, Phys. Rev. A **99**, 043602 (2019).
- [34] B. Dóra and R. Moessner, Phys. Rev. Lett. **119**, 026802 (2017).
- [35] N. Tsuji, P. Werner, and M. Ueda, Phys. Rev. A **95**, 011601(R) (2017).
- [36] C.-J. Lin and O. I. Motrunich, Phys. Rev. B **97**, 144304 (2018).
- [37] E. J. Torres-Herrera, A. M. García-García, and L. F. Santos, Phys. Rev. B **97**, 060303(R) (2018).
- [38] S. V. Syzranov, A. V. Gorshkov, and V. M. Galitski, Ann. Phys. (New York) **405**, 1 (2019).
- [39] M. McGinley, A. Nunnenkamp, and J. Knolle, Phys. Rev. Lett. **122**, 020603 (2019).
- [40] B. Swingle and D. Chowdhury, Phys. Rev. B **95**, 060201(R) (2017).
- [41] R. Fan, P. Zhang, H. Shen, and H. Zhai, Sci. Bull. **62**, 707 (2017).
- [42] X. Chen, T. Zhou, D. A. Huse, and E. Fradkin, Ann. Phys. (Berlin) **529**, 1600332 (2017).
- [43] R.-Q. He and Z.-Y. Lu, Phys. Rev. B **95**, 054201 (2017).
- [44] Y. Chen, arXiv:1608.02765.
- [45] Y. Huang, Y.-L. Zhang, and X. Chen, Ann. Phys. (Berlin) **529**, 1600318 (2017).
- [46] K. Slagle, Z. Bi, Y.-Z. You, and C. Xu, Phys. Rev. B **95**, 165136 (2017).
- [47] P. Bordia, F. Alet, and P. Hosur, Phys. Rev. A **97**, 030103(R) (2018).
- [48] J. Riddell and E. S. Sørensen, Phys. Rev. B **99**, 054205 (2019).
- [49] B. Swingle, G. Bentsen, M. Schleier-Smith, and P. Hayden, Phys. Rev. A **94**, 040302(R) (2016).
- [50] N. Y. Yao, F. Grusdt, B. Swingle, M. D. Lukin, D. M. Stamper-Kurn, J. E. Moore, and E. A. Demler, arXiv:1607.01801.
- [51] G. Zhu, M. Hafezi, and T. Grover, Phys. Rev. A **94**, 062329 (2016).
- [52] N. Yunger Halpern, Phys. Rev. A **95**, 012120 (2017).
- [53] N. Yunger Halpern, B. Swingle, and J. Dressel, Phys. Rev. A **97**, 042105 (2018).
- [54] J. Dressel, J. R. González Alonso, M. Waegell, and N. Yunger Halpern, Phys. Rev. A **98**, 012132 (2018).
- [55] J. Li, R. Fan, H. Wang, B. Ye, B. Zeng, H. Zhai, X. Peng, and J. Du, Phys. Rev. X **7**, 031011 (2017).
- [56] M. Gärttner, J. G. Bohnet, A. Safavi-Naini, M. L. Wall, J. J. Bollinger, and A. M. Rey, Nat. Phys. **13**, 781 (2017).
- [57] E. J. Meier, J. Ang'ong'a, F. A. An, and B. Gadway, arXiv:1705.06714.
- [58] D. M. Basko, I. L. Aleiner, and B. L. Altshuler, Ann. Phys. (New York) **321**, 1126 (2006).
- [59] V. Oganesyan and D. A. Huse, Phys. Rev. B **75**, 155111 (2007).
- [60] R. Nandkishore and D. A. Huse, Annu. Rev. Condens. Matter Phys. **6**, 15 (2015).
- [61] E. Altman and R. Vosk, Annu. Rev. Condens. Matter Phys. **6**, 383 (2015).
- [62] P. W. Anderson, Phys. Rev. **109**, 1492 (1958).
- [63] M. Serbyn, M. Knap, S. Gopalakrishnan, Z. Papić, N. Y. Yao, C. R. Laumann, D. A. Abanin, M. D. Lukin, and E. A. Demler, Phys. Rev. Lett. **113**, 147204 (2014).
- [64] M. Serbyn, Z. Papić, and D. A. Abanin, Phys. Rev. B **90**, 174302 (2014).
- [65] R. Vasseur, S. A. Parameswaran, and J. E. Moore, Phys. Rev. B **91**, 140202(R) (2015).
- [66] M. Serbyn and D. A. Abanin, Phys. Rev. B **96**, 014202 (2017).
- [67] M. Serbyn, Z. Papić, and D. A. Abanin, Phys. Rev. Lett. **111**, 127201 (2013).
- [68] D. A. Huse, R. Nandkishore and V. Oganesyan, Phys. Rev. B **90**, 174202 (2014).
- [69] J. Z. Imbrie, J. Stat. Phys. **163**, 998 (2016).
- [70] A. Pal and D. A. Huse, Phys. Rev. B **82**, 174411 (2010).
- [71] M. Žnidarič, T. Prosen, and P. Prelovšek, Phys. Rev. B **77**, 064426 (2008).

- [72] J. H. Bardarson, F. Pollmann, and J. E. Moore, Phys. Rev. Lett. **109**, 017202 (2012).
- [73] A. De Luca and A. Scardicchio, Europhys. Lett. **101**, 37003 (2013).
- [74] D. J. Luitz, N. Laflorencie, and F. Alet, Phys. Rev. B **91**, 081103(R) (2015).
- [75] A. Nanduri, H. Kim, and D. A. Huse, Phys. Rev. B **90**, 064201 (2014).